Activation of AMP-activated protein kinase decreases receptor activator of NF-κB ligand expression and increases sclerostin expression by inhibiting the mevalonate pathway in osteocytic MLO-Y4 cells

Maki Yokomoto-Umakoshi, Ippei Kanazawa, Ayumu Takeno, Ken-ichiro Tanaka, Masakazu Notsu, and Toshitsugu Sugimoto

Internal Medicine 1, Shimane University Faculty of Medicine, 89-1, Enya-cho, Izumo, Shimane, 693-8501, Japan

E-mail addresses: Maki Yokomoto; pinyan@med.shimane-u.ac.jp

Ippei Kanazawa; ippei.k@med.shimane-u.ac.jp

Ayumu Takeno; atakeno@med.shimane-u.ac.jp

Ken-ichiro Tanaka; ken1nai@med.shimane-u.ac.jp

Masakazu Notsu; mnotsu25@med.shimane-u.ac.jp

Toshitsugu Sugimoto; sugimoto@med.shimane-u.ac.jp

Correspondence and requests for reprints:

Ippei Kanazawa, MD, PhD

Internal Medicine 1, Shimane University Faculty of Medicine, 89-1, Enya-cho, Izumo, Shimane, 693-8501, Japan

Phone: +81-853-20-2183, Fax: +81-853-23-8650

E-mail: ippei.k@med.shimane-u.ac.jp

Number of words: abstract, 173 words; manuscript, 2289 words

Number of tables: 0

Number of figures: 4

Grants: This study was partly supported by a Grant-in-Aid for Scientific Research (C) (15K09433).

Disclosure Summary: The authors have nothing to disclose.

Abstract

Background: AMP-activated protein kinase (AMPK) plays important roles in bone metabolism; however, little is known about its role in osteocytes. This study investigated the effects of AMPK activation on the expression of receptor activator of NF-κB ligand (RANKL) and sclerostin in osteocytes.

Results: Real-time PCR showed that AMPK activation by 5-aminoimidazole-4-carboxamide ribonucleotide (AICAR) significantly decreased the expression of *Rankl* in a dose- and time-dependent manner and significantly increased the expression of *Sost*, the gene encoding sclerostin, in osteocytic MLO-Y4 cells. Western blotting confirmed that AICAR decreased RANKL protein levels and increased sclerostin levels. In addition, suppression of AMPKα1 by siRNA significantly increased the expression of *Rankl* on 4 days after the transfection of siRNA, while *Sost* expression was not changed. Simvastatin, an inhibitor of HMG-CoA reductase, significantly decreased *Rankl* expression and increased *Sost* expression in MLO-Y4 cells. Supplementation with mevalonate or geranylgeranyl pyrophosphate, which are downstream metabolites of HMG-CoA reductase, significantly reversed the effects of AICAR.

Conclusion: These findings indicated that AMPK regulated RANKL and sclerostin

expression through the mevalonate pathway in osteocytes.

Key words: AMP-activated protein kinase; osteocyte; RANKL; sclerostin; mevalonate pathway

Introduction

Bone tissue is constantly renewed by a balanced between bone formation and bone resorption. Several studies have shown that osteocytes play multifunctional roles in orchestrating bone remodeling by regulating both osteoblast and osteoclast functions [1,2]. A recent study showed that osteocytes expressed much higher levels of receptor activator of nuclear factor-κB ligand (RANKL) and had a great capacity to support osteoclastogenesis [3]. Previous studies have indicated that osteocyte-derived RANKL plays a key role in bone remodeling in response to mechanical loading [3-5]. Thus, osteocytes are the main cells involved in the initiation of bone remodeling. In addition, osteocytes produce osteoprotegerin (OPG), a decoy receptor for RANKL. Thus, osteocytes regulate bone resorption by regulating RANKL/OPG ratio [2]. Osteocytes also produce sclerostin, a protein encoded by *Sost*, that inhibits osteoblast activity by blocking Wnt/beta-catenin pathway [6,7].

AMP-activated protein kinase (AMPK) is a crucial regulator of energy and metabolic homeostasis at the cellular and whole-organism levels [8,9]. AMPK is a heterotrimeric complex containing a catalytic α subunit and regulatory β and γ subunits and functions as a serine/threonine kinase [10]. An increase in cellular AMP/ATP ratio activates AMPK through the phosphorylation of the α subunit (Thr 172). Once activated,

AMPK inactivates several metabolic enzymes involved in ATP-consuming cellular events, including cholesterol and protein synthesis, by inhibiting HMG-CoA reductase [11].

Increasing evidence indicates that osteoporosis is a disorder of energy metabolism. Recent studies have shown that the AMPK signaling pathway plays pivotal roles in bone physiology [12]. AMPK subunits are expressed in bone tissue and cells, with AMPKα1 subunit being the dominant catalytic isoform expressed in the bone [13]. A study showed that mice lacking the AMPKα1 subunit (AMPKα1$^{-/-}$ mice) experienced a significant reduction in bone mass [14], suggesting that this subunit played a major role in skeletal metabolism. Activated AMPK inhibits osteoclast formation and bone resorption in vitro [15]. We previously showed that AMPK activation stimulated the differentiation and mineralization of osteoblastic MC3T3-E1 cells by inhibiting mevalonate pathway [16-18]. Moreover, we recently reported that AMPK activation exerted protective effects against homocysteine-induced apoptosis of osteocytic MLO-Y4 cells [19].

However, the effects of AMPK activation on RANKL and sclerostin expression in osteocytes are unclear. This is the first study to show that AMPK activation by 5-aminoimidazole-4-carboxamide ribonucleotide (AICAR) decreased RANKL

expression and increased sclerostin expression by inhibiting the mevalonate pathway in osteocytic MLO-Y4 cells.

Materials and methods

Reagents

Cell culture medium and supplements were purchased from Gibco-BRL (Rockville, MD). AICAR and antibodies against total AMPKα and phosphorylated AMPKα were purchased from Cell Signaling (Beverly, MA). Antibodies against AMPKα1 and α2 subunits were purchased from Abcam (Tokyo, Japan). Simvastatin, mevalonate, and geranylgeranyl pyrophosphate (GGPP) were purchased from Sigma–Aldrich (St. Louis, MO). Antibodies against RANKL and sclerostin were purchased from Santa Cruz Biotechnology (Santa Cruz, CA) and Abcam, respectively. Rabbit monoclonal antibodies were purchased from Sigma–Aldrich. All other chemicals were of the highest grade available commercially.

Cell cultures

MLO-Y4 cell line, a murine long bone-derived osteocytic cell line, was kindly provided by Dr. Lynda F. Bonewald. MLO-Y4 cells were cultured on collagen-coated plates in α-minimum essential medium supplemented with 10% fetal bovine serum and 1% penicillin–streptomycin in 5% CO_2 at 37°C. The medium was changed twice a week, and the cells were passaged after they reached 80% confluency.

Reverse transcription–PCR to identify the AMPKα1 subunit

The mRNA expression of the AMPKα1 subunit in MLO-Y4 cells was determined by performing reverse transcription (RT)–PCR. Total RNA was extracted from the cultured MLO-Y4 cells by using TRIzol reagent (Invitrogen, San Diego, CA), according to the manufacturer's recommended protocol. In all, 2 μg of the total RNA was used for synthesizing single-stranded cDNA (cDNA synthesis kit; Invitrogen). PCR conditions were as follows: 35 cycles of denaturation at 95°C for 45 s, annealing at 60°C, and elongation at 72°C for 1 min. PCR products were electrophoresed on a 1.8% agarose gel stained with ethidium bromide and were visualized under ultraviolet (UV) light by using an electronic UV transilluminator (Toyobo Co. Ltd., Tokyo, Japan).

Quantification of gene expression by performing real-time PCR

SYBR green chemistry was used to determine the mRNA levels of *Rankl*, *Opg*, *Sost*, and *36B4*, a housekeeping gene. The following primers were used: *Rankl* forward, 5′-CACCATCAGCTGAAGATAGT-3′ and *Rankl* reverse, 5′-CCAAGATCTCTAACATGACG-3′; *Opg* forward, 5′-AGCTGCTGAAGCTGTGGAA-3′ and *Opg* reverse,

5′-TGTTCGAGTGGCCGAGAT-3′; *Sost* forward, 5′-GGAATGATGCCACAGAGGTCAT-3′ and *Sost* reverse, 5′-CCCGGTTCATGGTCTGGTT-3′; and *36B4* forward, 5′-AAGCGCGTCCTGGCATTGTCT-3′ and *36B4* reverse, 5′-CCGCAGGGGCAGCAGTGGT-3′. Real-time PCR was performed in a 25-μL reaction mixture containing 1 μL cDNA by using ABI PRISM 7000 (Applied Biosystems, Waltham, MA). Double-stranded DNA-specific SYBR Green I was mixed with PCR buffer provided in SYBR Green Real-Time PCR Master Mix (Toyobo Co. Ltd.) to quantify the PCR products. PCR conditions were as follows: initial denaturation at 95°C for 15 min and 40 cycles of denaturation at 94°C for 15 s and annealing and extension at 60°C for 1 min. The mRNA level of *36B4* was used to normalize the differences in the efficiency of RT.

Western blotting

For western blotting, the cells were plated in 6-well plates and were cultured as described above. After reaching confluency, the cells were treated with each agent for 48 h. The cells were then rinsed with ice-cold PBS and were scraped on ice in lysis buffer (65.8 mM Tris–HCl [pH 6.8], 26.3% [w/v] glycerol, 2.1% SDS, and 0.01%

bromophenol blue; Bio-Rad, Hercules, CA) supplemented with 2-mercaptoethanol at a final concentration of 5%. The cell lysates were sonicated for 20 s and were electrophoresed by performing SDS-PAGE on a 10% polyacrylamide gel. The separated proteins were transferred onto a nitrocellulose membrane (Bio-Rad). The membrane was blocked with TBS containing 1% Tween 20 (Bio-Rad) and 3% bovine serum albumin for 1 h at 4°C and was incubated overnight with specific antibodies at 4°C with gentle shaking. The membrane was then extensively washed with TBS containing 1% Tween 20 and was incubated with horseradish peroxidase-coupled rabbit anti-mouse antibody in TBS for 30 min at 4°C. The membrane was washed, and signals were detected using an enhanced chemiluminescence technique.

RNA interference for AMPKα subunits

RNA interference was used to down-regulate the expression of AMPKα subunit in MLO-Y4 cells. SMARTpool small interfering RNA (siRNA) and SMARTpool reagents for AMPKα1, AMPKα2 and nonspecific control siRNA duplexes were designed and synthesized by Customer SMARTpool siRNA Design from Dharmacon (Lafayette, CO). For gene knock down experiments, MLO-Y4 cells were plated in 6 cm dish and cultured for 48 h in α-MEM containing 10% FBS and

antibiotics. Next, after 24 h incubation in medium without antibiotics, cells were transfected with siRNAs (50 nM) using transfection reagent according to the manufacture's instructions. After another 48 h of culture, cells were recultured in another in α-MEM containing 10% FBS and antibiotics.

Statistical analysis

Results are expressed as mean ± standard error (SE). Statistical differences between groups were determined using one-way ANOVA followed by Fisher's protected least significant difference. For all statistical tests, a p value of <0.05 was considered statistically significant.

Results

AMPK activation increases RANKL expression and decreases Sost expression in MLO-Y4 cells

We have previously shown that all AMPK subunits are expressed in MLO-Y4 cells [19]. In this study, we confirmed the mRNA expression of the AMPKα1 and AMPKα2 subunits, the catalytic subunit (Fig. 1A). Moreover, the protein levels of AMPKα1 and AMPKα2 subunits were examined in mouse stromal ST2, mouse osteoblast-like MC3T3-E1, and MLO-Y4 cells (Fig. 1B). The protein expression of AMPKα2 was relatively low in MLO-Y4 cells compared to other cells. We also confirmed that 1.0 mM AICAR treatment phosphorylated AMPKα subunit until 3 hours (Fig. 1C).

After reaching confluency, the MLO-Y4 cells were treated with AICAR for 48 h and total RNA was collected. Real-time PCR showed that AICAR significantly decreased *Rankl* expression and *Rankl*/*Opg* ratio in a dose-dependent manner (Fig. 2A and 2C) but did not affect *Opg* expression (Fig. 2B). In contrast, AICAR treatment significantly increased *Sost* expression in a dose-dependent manner (Fig. 2D). Next, we examined the time-dependent effects of AICAR during 48-h treatment. We observed that *Rankl* expression and *Rankl*/*Opg* ratio were significantly decreased in a

time-dependent manner and that *Sost* expression peaked after 24 h of treatment (Fig. 2E–H). However, AICAR treatment did not affect *Opg* expression at any time point.

Western blotting showed that 72-h treatment with AICAR suppressed RANKL protein expression in a dose-dependent manner (Fig. 2I) and increased sclerostin expression (Fig. 2J).

Next, to examine the effects of AMPKα subunits knockdown on MLO-Y4 cells, we investigated the expression of *Rankl* and *Sost* in the siRNA-transfected cells. The total RNA was collected on 4 days after the siRNA treatment. Real-time PCR showed increased *Rankl* expression by the siRNA-AMPKα1 (Fig. 3B), but not siRNA-AMPKα2 (Fig. 3C). On the other hand, the expression of *Sost* was not significantly affected by the siRNA-AMPKα1 or siRNA-AMPKα2 (Fig. 3D and E).

AMPK activation decreases Rankl expression and increases Sost expression by inhibiting the mevalonate pathway in MLO-Y4 cells

To examine whether the mevalonate pathway was involved in the effects of AMPK activation, we examined the effects of simvastatin on the expression of *Rankl* and *Sost*. Real-time PCR showed that treatment of MLO-Y4 cells with 1.0 μM simvastatin significantly decreased *Rankl* expression (Fig. 4A) and increased *Sost*

expression (Fig. 4B), which was similar to that observed after treatment with 0.5–1.0 mM AICAR. Moreover, co-incubation with 1.0 mM mevalonate or 5.0 μM GGPP, the immediate downstream metabolites of HMG-CoA reductase, significantly reversed AICAR-suppressed *Rankl* expression (Fig. 4C) and AICAR-augmented *Sost* expression (Fig. 4D). However, mevalonate or GGPP did not affect *Rankl* or *Sost* expression in the absence of AICAR.

Discussion

We recently showed that AMPK subunits are expressed in osteocytic MLO-Y4 cells and that AMPK exerts antiapoptotic effects against homocysteine-induced oxidative stress in these cells [19]. In the present study, we confirmed that expression of the AMPKα1 and AMPKα2 subunits was maintained during the 14-day and that this subunit was phosphorylated by AICAR. Moreover, we observed that AMPK activation regulated RANKL and *Sost* expression in MLO-Y4 cells, suggesting that AMPK plays important roles in bone metabolism.

A previous study showed that deletion of the AMPKα1 subunit ($AMPK\alpha1^{-/-}$) decreased bone mass in vivo [20]. In addition, dynamic bone histomorphometric analysis showed high bone turnover in $AMPK\alpha1^{-/-}$ mice compared with that in their $AMPK\alpha1^{+/+}$ littermates, suggesting increased bone resorption [20]. These findings suggest that AMPK plays a pivotal role in bone remodeling. Although previous studies have shown that AMPK activation directly inhibits osteoclastogenesis [15,21], Mai et al. reported that AMPK activation by metformin indirectly suppresses osteoclast differentiation by stimulating OPG and reducing RANKL expression in osteoblasts [22]. Because we found that AMPK was expressed in osteocytes, we hypothesized that AMPK activation affected RANKL and OPG expression in osteocytes to regulate

osteoclast activity. We found that AICAR activation significantly decreased RANKL expression in MLO-Y4 cells in a dose- and time-dependent manner, and that knockdown of AMPKα1 significantly increased RANKL expression. These findings suggested that AMPK activation inhibited osteoclast activity by decreasing RANKL expression in both osteoblasts and osteocytes, which is in accordance with the findings of an in vivo study involving AMPKα1$^{-/-}$ mice [14].

We and other investigators have previously shown that activated AMPK stimulates the differentiation and mineralization of osteoblasts [16-18,23-26], suggesting that AMPK activation stimulates bone formation in vivo. However, AMPKα1$^{-/-}$ mice did not show a significant alteration in bone formation rate compared with control mice [14]. This discrepancy between in vitro and in vivo studies might be explained by the finding of the present study that activated AMPK increases sclerostin expression in osteocytic MLO-Y4 cells. Therefore, it can be suggested that AMPK directly stimulates osteoblastic differentiation and negatively affects osteoblasts by increasing sclerostin expression in osteocytes through negative feedback regulation. However, the effect of AICAR on the increased *Sost* mRNA was temporal, and the mRNA expression level was not changed by knockdown of AMPKα, suggesting that the role of AMPK in regulation of sclerostin expression may be trivial.

The mevalonate pathway plays a crucial role in bone metabolism [27,28]. HMG-CoA reductase acts in the rate-limiting step of cholesterol synthesis and statins, which are pharmacological inhibitors of HMG-CoA reductase, block the conversion of HMG-CoA to mevalonate [29]. Mundy et al. were the first to report that statins stimulate bone formation in rodents and increase new bone volume in cultures of mouse calvaria [30]. Other investigators have also suggested that statins inhibit osteoclast activation, thus suppressing bone resorption [27,31]. However, to our knowledge, none of these studies have examined the role of the mevalonate pathway in osteocytes thus far. We previously reported that AMPK activation stimulated the differentiation and mineralization of osteoblastic MC3T3-E1 cells by suppressing the mevalonate pathway [17]. In the present study, we observed that simvastatin significantly decreased RANKL expression and increased *Sost* expression and that mevalonate or GGPP, the immediate downstream metabolites of HMG-CoA reductase, significantly reversed AICAR-suppressed RANKL expression and AICAR-augmented *Sost* expression. These findings indicate that the mevalonate pathway plays important roles in regulating bone remodeling and that AMPK activation decreases RANKL expression and increases sclerostin expression by inhibiting HMG-CoA reductase in osteocytes.

In conclusion, this is the first study to show that AMPK activation decreased

RANKL expression and increased sclerostin expression by inhibiting the mevalonate pathway in osteocytic MLO-Y4 cells. Further studies on the role of AMPK in osteocytes would provide new insights on the effects of AMPK on bone metabolism.

Acknowledgements

This study was partly supported by a Grant-in-Aid for Scientific Research (C) (15K09433). Authors' roles: Study design and conduct: MY and IK. Performed the experiments and analyzed the data: MY and AT. Contributed equipment/materials: IK, MN, KT, and TS. Wrote the paper: MY and IK. Approving final version: all authors. IK takes responsibility for the integrity of the data analysis. The authors thank Keiko Nagira for technical assistance.

Conflicts of interest

None.

References

1. S.L. Dallas, M. Prideaux, L.F. Bonewald. The osteocyte: an endocrine cell… and more. Endocr Rev 2013;34: 658-90.

2. L.F. Bonewald. The amazing osteocyte. J Bone Miner Res 2011; 26: 229-38.

3. T. Nakashima, M. Hayashi, T. Fukunaga, K. Kurata, M. Oh-Hora, J.Q. Feng, L.F. Boneward, T. Kodama, A. Wutz, E.F. Wagner, J.M. Penninger, H. Takayanagi. Evidence for osteocyte regulation of bone homeostasis through RANKL expression. Nature Med 2011; 17: 1231-4.

4. T. Nakashima, M. Hayashi, H. Takayanagi. New insights into osteoclastogenic signaling mechanisms. Trends Endocrinol Metab 2012; 23: 582-90.

5. M. Honma, Y. Ikebuchi, Y. Kariya, M. Hayashi, N. Hayashi, S. Aoki, H. Suzuki. RANKL subcellular trafficking and regulatory mechanisms in osteocytes. J Bone Miner Res 2013; 28: 1936-49.

6. T.A. Burgers, B.O. Williams. Regulation of Wnt/β-catenin signaling within and from osteocytes. Bone 2013; 54: 244-9.

7. X. Li, Y. Zhang, H. Kang, W. Liu, P. Liu, J. Zhang, S.E. Harris, D. Wu. Sclerostin binds to LRP5/6 and antagonizes canonical Wnt signaling. J Biol Chem 2005; 280: 19883-7.

8. B.B. Kahn, T. Alquier, D. Carling, D.G. Hardie. AMP-activated protein kinase:

ancient energy gauge provides clues to modern understanding of metabolism. Cell Metab 2005; 1: 15-25.

9. N.B. Ruderman, D. Carling, M. Prentki, J.M. Cacicedo. AMPK, insulin resistance, and the metabolic syndrome. J Clin Invest 2013; 123: 2764-72.

10. A. Salminen, J.M. Hyttinen, K. Kaarniranta. AMP-activated protein kinase inhibits NF-κB signaling and inflammation: impact on health span and lifespan, J Mol Med 2011; 89: 667-76.

11. H. Motoshima, B.J. Goldstein, M. Igata, E. Araki. AMPK and cell proliferation-AMPK as a therapeutic target for atherosclerosis and cancer. J Physiol 2006; 574: 63-71.

12. J. Jeyabalan, M. Shah, B. Viollet, C. Chenu. AMP-activated protein kinase pathway and bone metabolism. J Endocrinol 2012; 212: 277-90.

13. J.M. Quinn, S. Tam, N.A. Sims, H. Saleh, N.E. McGregor, I.J. Poulton, J.W. Scott, M.T. Gillespie, B.E. Kemp, B.J. van Denderen. Germline deletion of AMP-activated protein kinase beta subunits reduces bone mass without altering osteoclast differentiation or function. FASEB J 2010; 24: 275-85.

14. M. Shah, B. Kola, A. Bataveljic, T.R. Arnett, B. Viollet, L. Saxon, M. Korbonits, C. Chenu. AMP-activated protein kinase (AMPK) activation regulates in vitro bone

formation and bone mass. Bone 2010; 47: 309-19.

15. Y.S. Lee, Y.S. Kim, S.Y. Lee, G.H. Kim, B.J. Kim, S.H. Lee, K.U. Lee, G.S. Kim, S.W. Kim, J.M. Koh. AMP kinase acts as a negative regulator of RANKL in the differentiation of osteoclasts. Bone 2010; 47: 926-37.
16. I. Kanazawa, T. Yamaguchi, S. Yano, M. Yamauchi, T. Sugimoto. Metformin enhances the differentiation and mineralization of osteoblastic MC3T3-E1 cells via AMP kinase activation as well as eNOS and BMP-2 expression. Biochem Biophys Res Commun 2008; 375: 414-9.
17. I. Kanazawa, T. Yamaguchi, S. Yano, M. Yamauchi, T. Sugimoto. Activation of AMP kinase and inhibition of Rho kinase induce the mineralization of osteoblastic MC3T3-E1 cells through endothelial NOS and BMP-2 expression. Am J Physiol Endocrinol Metab 2009; 296: E139-46.
18. I. Kanazawa, T. Yamaguchi, S. Yano, M. Yamauchi, M. Yamamoto, T. Sugimoto. Adiponectin and AMP kinase activator stimulate proliferation, differentiation, and mineralization of osteoblastic MC3T3-E1 cells. BMC Cell Biol 2007; 8: 51.
19. A. Takeno, I. Kanazawa, K. Tanaka, M. Notsu, M. Yokomoto, T. Yamaguchi, T. Sugimoto. Activation of AMP-activated protein kinase protects against homocysteine-induced apoptosis of osteocytic MLO-Y4 cells by regulating the

expressions of NADPH oxidase 1 (Nox1) and Nox2. Bone 2015; 77: 135-41.

20. J. Jeyabalan, M. Shah, B. Viollet, J.P. Roux, P. Chavassieux, M. Korbonits, C. Chenu. Mice lacking AMP-activated protein kinase α1 catalytic subunit have increased bone remodelling and modified skeletal responses to hormonal challenges induced by ovariectomy and intermittent PTH treatment. J Endocrinol 2012; 214: 349-58.
21. H. Kang, B. Viollet, D. Wu. Genetic deletion of catalytic subunits of AMP-activated protein kinase increases osteoclasts and reduces bone mass in young adult mice. J Biol Chem 2013; 288: 12187-96.
22. Q.G. Mai, Z.M. Zhang, S. Xu, M. Lu, R.P. Zhou, L. Zhao, C.H. Jia, Z.H. Wen, D.D. Jin, X.C. Bai. Metformin stimulates osteoprotegerin and reduces RANKL expression in osteoblasts and ovariectomized rats. J Cell Biochem 2011; 112: 2902-9.
23. A.M. Cortizo, C. Sedlinsky, A.D. McCarthy, A. Blanco, L. Schurman. Osteogenic actions of the anti-diabetic drug metformin on osteoblasts in culture. Eur J Pharmacol 2006; 536: 38-46.
24. A. Pantovic, A. Krstic, K. Janjetovic, J. Kocic, L. Harhaji-Trajkovic, D. Bugarski, V. Trajkovic. Coordinated time-dependent modulation of AMPK/Akt/mTOR signaling

and autophagy controls osteogenic differentiation of human mesenchymal stem cells. Bone 2013; 52: 524-31.

25. W.G. Jang, E.J. Kim, K.N. Lee, H.J. Son, J.T. Koh. AMP-activated protein kinase (AMPK) positively regulates osteoblast differentiation via induction of Dlx5-dependent Runx2 expression in MC3T3E1 cells. Biochem Biophys Res Commun 2011; 404: 1004-9.
26. M.S. Molinuevo, L. Schurman, A.D. McCarthy, A.M. Cortizo, M.J. Tolosa, M.V. Gangoiti, V. Arnol, C. Sedlinsky. Effect of metformin on bone marrow progenitor cell differentiation: in vivo and in vitro studies. J Bone Miner Res 2010;25: 211-21.
27. M. Yamashita, F. Otsuka, T. Mukai, R. Yamanaka, H. Otani, Y. Matsumoto, E. Nakamura, M. Takano, K.E. Sada, H. Makino. Simvastatin inhibits osteoclast differentiation induced by bone morphogenetic protein-2 and RANKL through regulating MAPK, AKT and Src signaling. Regul Pept 2010; 162: 99-108.
28. N. Horiuchi, T. Maeda. Statins and bone metabolism. Oral Dis 2006; 12: 85-101.
29. A. Barszczyk, H.S. Sun, Y. Quan, W. Zheng, M.P. Charlton, Z.P. Feng. Differential roles of the mevalonate pathway in the development and survival of mouse purkinje cells in culture. Mol Neurobiol 2015; 51: 1116-29.
30. G. Mundy, R. Garrett, S. Harris, J. Chan, D. Chen, G. Rossini, B. Boyce, M. Zhao,

G. Gutierrez. Stimulation of bone formation in vitro and in rodents by statins. Science 1999; 286: 1946-9.

31. W.A. Grasser, A.P. Baumann, S.F. Petras, H.J. Harwood Jr, R. Devalaraja, R. Renkiewicz, V. Baragi, D.D. Thompson, V.M. Paraklar. Regulation of osteoclast differentiation by statins. J Musculoskelet Neuronal Interact 2003;3: 53-62.

Figure legends

Fig. 1. Expression and phosphorylation of the AMPKα1 subunit in MLO-Y4 cells.

Total RNA extracted from MLO-Y4 cells was subjected to RT–PCR, and PCR products were visualized by performing electrophoresis on a 1.8% agarose gel stained with ethidium bromide. The mRNA expression of the AMPKα1 and AMPKα2 subunits (A). Total proteins were extracted from mouse stromal ST2, mouse osteoblastic MC3T3-E1, and MLO-Y4 cells when the cells reached confluency. The protein levels of AMPKα1 and AMPKα2 subunits were detected by Western blotting (B). The cells were treated with 1.0 mM AICAR for 3 h, and whole cell lysates were collected on the indicated time points. Western blotting showed that AICAR phosphorylated the AMPKα subunit (C). The results are representative of 3 independent experiments.

Fig. 2. Effects of AMPK activation on the mRNA expression of *Rankl*, *Opg*, and *Sost* in MLO-Y4 cells.

Dose-dependent effects of 0.1–1.0 mM AICAR on the mRNA expression of RANKL, OPG, and *Sost* and *Rankl*/*Opg* ratio were examined (A–D). *Rankl* expression was significantly decreased in cells treated with 0.5 and 1.0 mM AICAR compared with that in control cells and cells treated with 0.1 mM AICAR (A). *Opg* expression was not

altered (B). *Rankl*/*Opg* ratio was significantly decreased in cells treated with 0.5 and 1.0 mM AICAR compared with that in control cells (C). *Sost* expression was significantly increased in cells treated with 1.0 mM AICAR treatment compared with that in control cells and cells treated with 0.1 and 0.5 mM AICAR (D). The results are expressed as mean ± SE of fold increase over control values ($n \geq 4$); $*p < 0.05$, $**p < 0.01$, $***p < 0.001$.

Time-dependent effects of 1.0 mM AICAR on *Rankl*, *Opg*, and *Sost* expression and *Rankl*/*Opg* ratio were determined (E–H). AICAR treatment significantly decreased *Rankl* expression and *Rankl*/*Opg* ratio in a time-dependent manner (E and G); however, *Opg* expression was unchanged (F). *Sost* expression was significantly increased after AICAR treatment and peaked at 24 h (H). The results are expressed as mean ± SE of fold increase over control values ($n \geq 5$); $*p < 0.05$, $**p < 0.01$, $***p < 0.001$ compared with 0 h.

MLO-Y4 cells were treated with the indicated concentrations of AICAR for 72 h, and whole cell lysates were collected. Western blotting showed that AICAR treatment decreased RANKL protein expression in a dose-dependent manner (I) and increased sclerostin expression (J). The results are representative of 3 independent experiments.

Fig. 3. Effects of siRNA-AMPKα1 or siRNA-AMPKα2 transfection on the expression of *Rankl* and *Sost* in MLO-Y4 cells

Total RNA was collected at 4 days after siRNA transfection. The effects of siRNA treatment were confirmed (A). N; no treatment, siα1; siRNA of AMPKα1, siα2; siRNA of AMPKα2, NC; transfection of non-targeting siRNA. *Rankl* mRNA expression was significantly decreased by knockdown of AMPKα1 (B), but not AMPKα2 (C). Sost mRNA expression was not changed (D and E). The results are expressed as mean ± SE of fold increase over control values ($n \geq 4$); $^{**}p < 0.01$.

Fig. 4. AMPK activation decreases *Rankl* expression and increases *Sost* expression by inhibiting the mevalonate pathway in MLO-Y4 cells

Treatment of MLO-Y4 cells with 0.5 and 1.0 mM AICAR and 1.0 μM simvastatin (SIM) for 48 h significantly decreased *Rankl* expression compared with that in control cells (A). The effect of SIM was similar to that of 0.5 mM AICAR. In contrast, treatment of MLO-Y4 cells with 1.0 mM AICAR and SIM significantly increased *Sost* expression compared with that in control cells (B). The effect of SIM was similar to that of 1.0 mM AICAR. The results are expressed as mean ± SE of fold increase over control values ($n \geq 4$); $^{*}p < 0.05$, $^{**}p < 0.01$, $^{***}p < 0.001$.

Addition of 1.0 mM mevalonate (MV) or 5.0 μM geranylgeranyl pyrophosphate (GGPP), the downstream metabolites of HMG-CoA reductase, reversed 1.0 mM AICAR-suppressed *Rankl* expression (C) and 1.0 mM AICAR-augmented *Sost* expression (D). The results are expressed as mean ± SE of fold increase over control values ($n \geq 5$); $*p < 0.05$, $**p < 0.01$, $***p < 0.001$.

Fig. 1

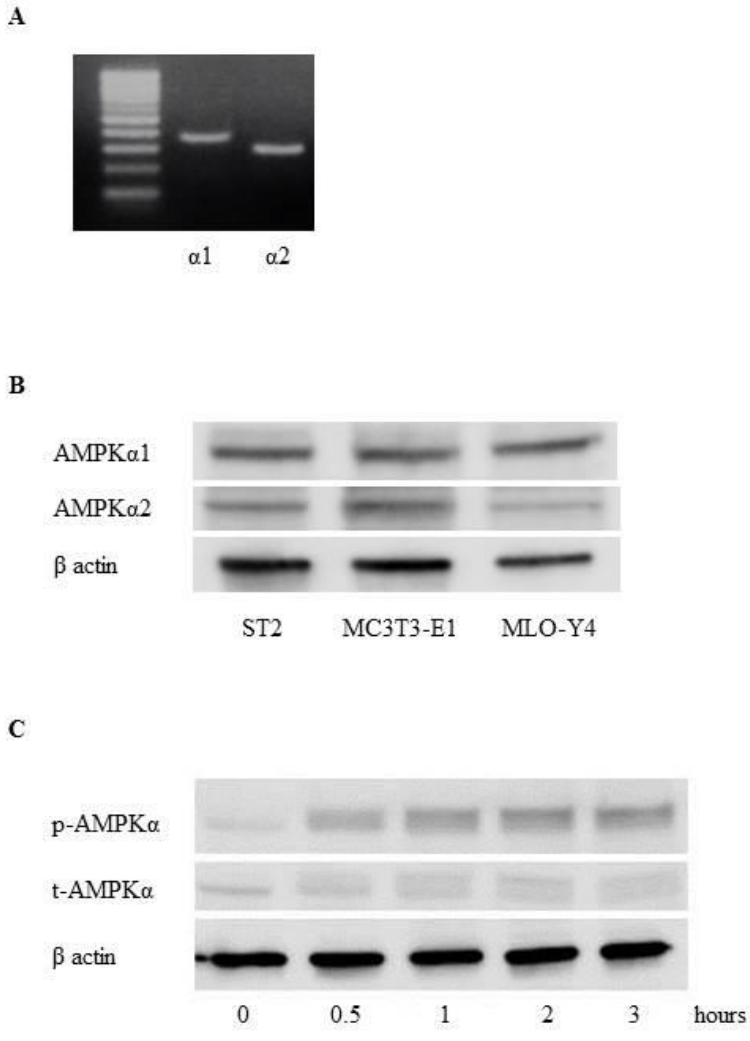
A
α1
α2
B
AMPKα1
AMPKα2
β actin
ST2
MC3T3-E1
MLO-Y4
C
p-AMPKα
t-AMPKα
β actin
0
0.5
1
2
3
hours

Fig. 2

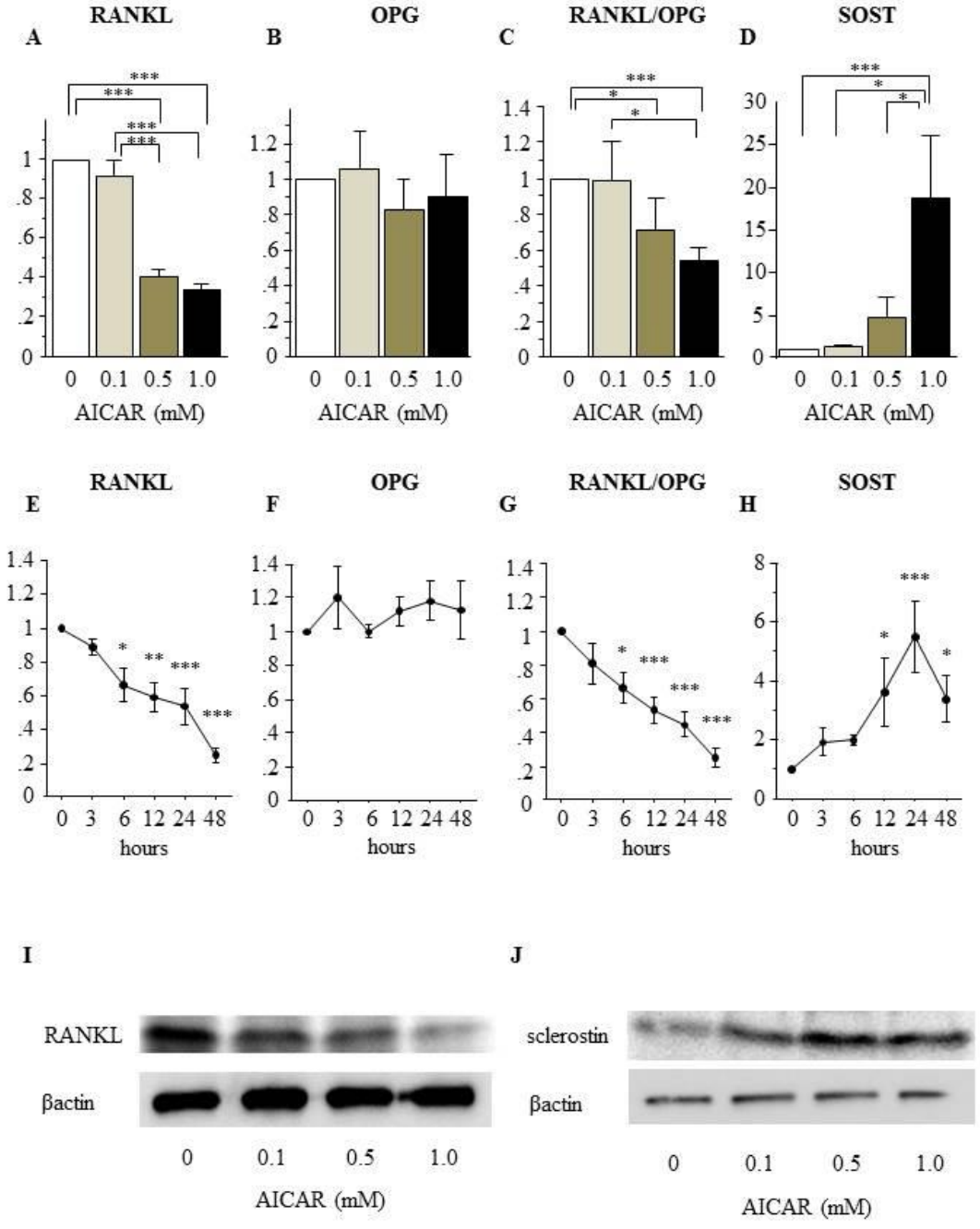
RANKL
A
OPG
B
RANKL/OPG
C
SOST
D
AICAR (mM)
0 0.1 0.5 1.0
RANKL
E
OPG
F
RANKL/OPG
G
SOST
H
hours
0 3 6 12 24 48
I
RANKL
βactin
AICAR (mM)
J
sclerostin
βactin
AICAR (mM)

Fig. 3

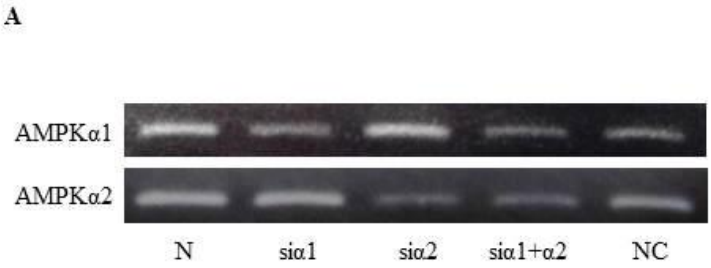
A
AMPKα1
AMPKα2
N
siα1
siα2
siα1+α2
NC

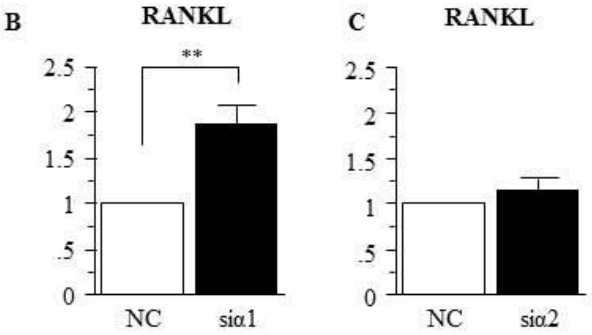
B
RANKL
**
2.5
2
1.5
1
.5
0
NC
siα1

C
RANKL
2.5
2
1.5
1
.5
0
NC
siα2

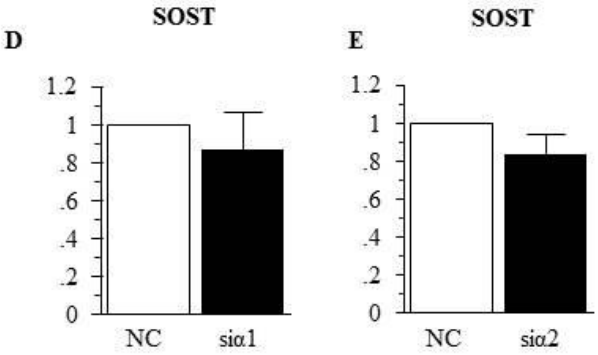
D
SOST
1.2
1
.8
.6
.4
.2
0
NC
siα1

E
SOST
1.2
1
.8
.6
.4
.2
0
NC
siα2

Fig. 4

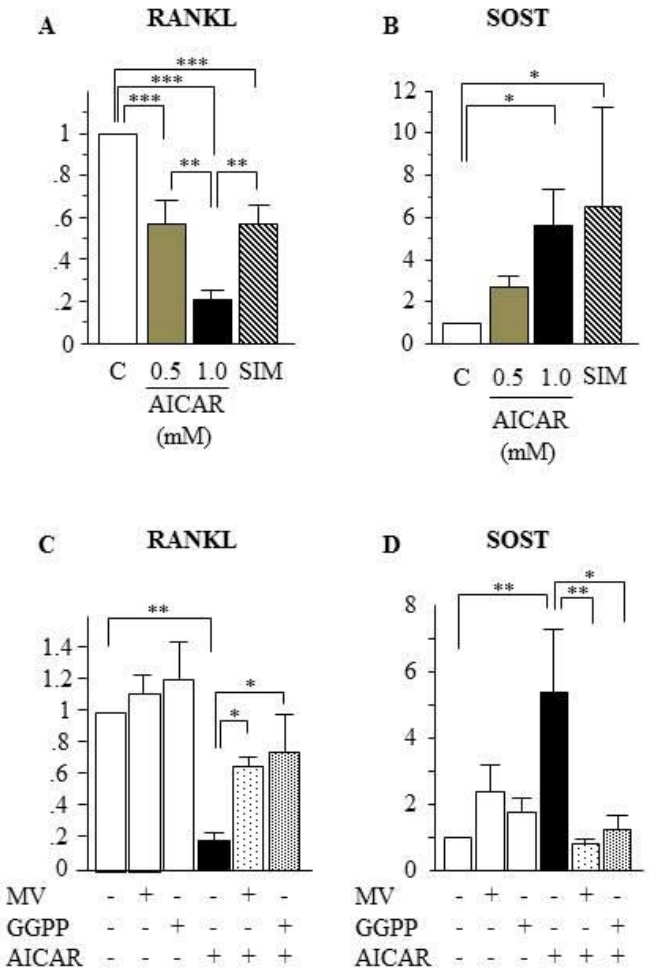
A
RANKL
***
***
***
**
**
1
.8
.6
.4
.2
0
C
0.5
1.0
SIM
AICAR
(mM)
B
SOST
*
*
12
10
8
6
4
2
0
C
0.5
1.0
SIM
AICAR
(mM)
C
RANKL
**
*
*
1.4
1.2
1
.8
.6
.4
.2
0
MV - + - - + -
GGPP - - + - - +
AICAR - - - + + +
D
SOST
**
**
*
8
6
4
2
0
MV - + - - + -
GGPP - - + - - +
AICAR - - - + + +